

Europium(III) and Its Halides in Anhydrous Room-Temperature Imidazolium-Based Ionic Liquids: A Combined TRES, EXAFS, and Molecular Dynamics Study

Clotilde Gaillard,^{*†} Isabelle Billard,[†] Alain Chaumont,[‡] Soufiane Mekki,[†] Ali Ouadi,[†] Melissa A. Denecke,[§] Gilles Moutiers,^{||} and Georges Wipff^{*‡}

Institut de Recherches Subatomiques, CNRS-IN2P3, B.P. 28, 67037 Strasbourg Cedex 2, France, Laboratoire MSM, UMR CNRS 7551, Institut de Chimie, 4 rue Blaise Pascal, 67000 Strasbourg, France, Forschungszentrum Karlsruhe GmbH, Institut für Nukleare Entsorgung, Postfach 3640, D-76021 Karlsruhe, Germany, and CEA Saclay, DEN/DPC/SCP/DIR, 91191 Gif-sur-Yvette Cedex, France

Received June 27, 2005

Combining spectroscopic techniques (TRES and EXAFS) and molecular dynamics simulations, we have investigated the state of trivalent europium dissolved in room-temperature ionic liquids (RTILs), as a function of the RTIL anion and in the presence of added chloride anions. The studied RTILs are based on the 1-butyl-3-methyl-imidazolium (Bumim⁺) cation and differ by their anionic counterparts: BF₄⁻, PF₆⁻, Tf⁻ (triflate, CF₃SO₃⁻), and Tf₂N⁻ [(CF₃SO₂)₂N⁻]. The results show the strong influence of the RTIL nature on the first solvation shell of europium and on its complexation with chloride. Depending on the RTIL, europium(III), which was introduced in solution as a triflate salt, is found to be solvated either by RTIL anions only or as neutral undissociated EuTf₃ moieties completed by solvent anions. Kinetic effects, related to the viscosity of the RTIL and the nature of the europium salt, also markedly influence the coordination of added Cl⁻ or F⁻ anions to the metal.

1. Introduction

Room-temperature ionic liquids (RTILs) have been extensively studied during the last 10 years in view of their applications in many fields of chemistry such as electrochemistry, separation, and synthesis.¹ The main interest in this class of solvents is related to their “green” properties (nonvolatile, nonflammable, etc.) but also from the variability of their physicochemical properties (stability, hydrophobicity, viscosity etc.), as a function of the RTIL cationic and anionic components. The combination of the commonly used 1-butyl-3-methyl-imidazolium cation (hereafter denoted Bumim⁺) with various inorganic anions results in air-, water-, temperature-, and radiation-stable RTILs, whereas their hydrophobicities or solvation abilities are controlled by the anion.^{2,3}

In the frame of nuclear fuel reprocessing, RTILs are particularly attractive in the improvement of existing processes or the development of new ones for actinide and lanthanide partitioning. The use of hydrophobic RTILs can be envisioned to replace toxic and volatile solvents used nowadays for actinide/lanthanide separation.^{4,5} Also, the design of task-specific ILs, i.e., RTILs in which a complexing moiety is grafted onto the cation skeleton, opens new routes for liquid/liquid extraction purposes.⁶ Metal electrodeposition from RTIL solutions appears to be also an interesting alternative for the separation/purification of nuclear wastes⁷ because recent electrochemical investigations have shown

* To whom correspondence should be addressed. E-mail: cgaillard@ires.in2p3.fr (C.G.), wipff@chimie.u-strasbg.fr (G.W.). Fax: 33.3.88.10.64.31 (C.G.), 33.3.90.24.15.45 (G.W.).

[†] CNRS-IN2P3.

[‡] Institut de Chimie.

[§] Institut für Nukleare Entsorgung.

^{||} CEA Saclay.

(1) Wasserscheid, P.; Welton, T. *Ionic liquids in synthesis*; Wiley-VCH: New York, 2003.

(2) Huddleston, J. G.; Visser, A. E.; Reichert, W. M.; Willauer, H. D.; Broker, G. A.; Rogers, R. D. *Green Chem.* **2001**, *3*, 156.

(3) Welton, T. *Chem. Rev.* **1999**, *99*, 2071.

(4) Visser, A. E.; Rogers, R. D. *J. Solid State Chem.* **2003**, *171*, 109.

(5) Gaillard, C.; Moutiers, G.; Mariet, C.; Antoun, T.; Gadenne, B.; Hesemann, P.; Moreau, J. J. E.; Ouadi, A.; Labet, A.; Billard, I. In *Ionic Liquids IIIB: Fundamentals, Progress, Challenges and Opportunities*; Rogers, R. D., Seddon, K. R., Eds.; Oxford University Press: Oxford, U.K., 2005.

(6) Visser, A. E.; Swatloski, R. P.; Reichert, W. M.; Mayton, R.; Sheff, S.; Wierzbicki, A.; Rogers, R. D. *Environ. Sci. Technol.* **2002**, *36*, 2523.

Table 1. Summary of the RTIL Solutions Analyzed by XAFS

RTIL	composition	[Cl]/[Eu] or [F]/[Eu] ratio	[Y ⁻]/[Cl ⁻] ratio ^a	sample ID ^b
BumimPF ₆	0.06 M EuTf ₃	0		“EuPF6”
	0.06 M EuTf ₃ + 0.35 M BumimCl	6	14	“EuCl6PF6”
	0.005 M EuTf ₃ + 0.03 M TBAF	6		“EuF6PF6”
BumimBF ₄	0.005 M EuTf ₃	0		“EuBF4”
	0.005 M EuTf ₃ + 0.03 M BumimCl	6	178	“EuCl6BF4”
BumimTf	0.005 M EuTf ₃	0		“EuTf”
	0.005 M EuTf ₃ + 0.03 M BumimCl	6	150	“EuCl6Tf”
BumimTf ₂ N	0.02 M EuTf ₃	0		“EuTf2N”
	0.02 M EuTf ₃ + BumimCl 0.12 M	6	29	“EuCl6Tf2N”
	0.01 M EuTf ₃ + BumimCl 0.09 M	9	38	“EuCl9Tf2N”

^a Y⁻ is the solvent anion. ^b Acronym under which the sample is referred to in the text.

that some RTILs exhibit good ionic conductivity over a wide electrochemical window compared to water or classical organic solvents.⁸

In this context, we have undertaken studies on the solvation and complexation of europium in Bumim RTILs. Eu(III) is chosen as a representative of lanthanides and as a homologue of trivalent actinides such as Am(III) and Cm(III). Our aim is to understand the solute/solution interactions in these unusual solvents. Our previous spectroscopic studies⁹ conducted in BumimTf₂N [Tf₂N⁻ = (CF₃SO₂)₂N⁻] highlighted the competitive role of water in the solvation of europium. By the addition of chloride ligands in solution, we also found evidence for the formation of polychloro complexes of europium, whose exact structure and stoichiometry could not be precisely determined. Theoretical approaches based on molecular dynamics (MD) simulations also pointed to the competition between solvent impurities (e.g., traces of water, halide ions, etc.) and RTIL ion components on the solvation of Eu(III) and uranyl cations.^{10,11}

The present work is an extended study on the solvation/complexation characteristics of Eu(III) in Bumim RTILs. The main focus is on the role of the RTILs' anionic part, which is expected to have a strong effect on the coordination properties of cationic species such as lanthanide ions. Time-resolved emission spectroscopy (TRES) and X-ray absorption fine structure (XAFS) spectroscopies (EXAFS and XANES) are used to characterize the solvation sphere of Eu(III) as a function of the anionic component of the RTIL: BumimBF₄, BumimPF₆, BumimTf (Tf⁻ = triflate, CF₃SO₃⁻), and BumimTf₂N. The complexes formed in each RTIL upon introduction of chloride ions ([Cl]/[Eu] = 6/1 and 9/1 in one case) are also investigated. The experimental results are complemented by MD simulations and quantum mechanical (QM) calculations on the solvation of “naked” Eu(III) cation and on its EuTf₃ complex in the BumimBF₄, BumimPF₆, and BumimTf₂N “pure” ILs. The effect of added Cl⁻ anions is also investigated by MD.

2. Methods

2.1. Chemicals. The RTILs BumimPF₆ and BumimTf₂N were synthesized and purified as previously reported.^{12,13} Their water contents after synthesis, measured by the Karl Fischer technique, were 0.7 M (9700 ppm) for BumimPF₆ and 0.6 M (8860 ppm) for BumimTf₂N. BumimTf and BumimBF₄ were purchased from Merck (purity ≥ 98% and water amount < 0.8 M). Organic impurities in these commercial RTILs make them colored, pale pink for BumimTf and yellow for BumimBF₄; our synthesized BumimPF₆ and BumimTf₂N are colorless. Impurities are also probably responsible for the low solubility of the europium salt observed in commercial BumimTf and BumimBF₄ (≈ 5 × 10⁻³ M). EuTf₃ (Aldrich) was used as received. Chloride ions were introduced into the solution as BumimCl, which was synthesized according to the procedure described in ref 13. Fluoride ions were introduced as tetrabutylammonium fluoride (TBAF; Aldrich).

For complexation studies in ILs, water must be considered as a competitive solute. It is thus necessary to control the amount of water in the solution. This may be achieved by degassing the solutions under vacuum and heat (e.g., at 70 °C and 1.8 mbar for 48 h).⁹ To optimize the degassing of the studied RTILs under vacuum (1.8 mbar), we tested three temperatures: at room temperature, at 70 °C, and at -180 °C (i.e., liquid N₂ temperature). Figure S1 (see the Supporting Information) displays the residual water amount in BumimTf₂N with time for these three temperatures. The RTIL water concentration was found to be below the detection limit of the Karl Fischer apparatus (100 ppm) after only 2 h of degassing, under vacuum at 70 °C, and at -180 °C. We selected the procedure at 70 °C and degassed each RTIL solution again after introduction of europium and chloride/fluoride salts. Thus, the maximum water concentration was 8 × 10⁻³ M, which corresponds to a H₂O/Eu ratio of 1:8 in the “EuPF6” sample, of less than 1:2 in “EuTf2N”, and ≈ 1 in the “EuBF4” and “EuTf” samples (defined in Table 1). Thus, any water complexation is expected to be either negligible or only a minority species.

Upon the addition of EuTf₃ to BumimTf₂N, a slightly cloudy solution was obtained, which indicates incomplete dissolution, likely involving the formation of inhomogeneous clusters. This cloudy solution strongly scattered red light of a He:Ne laser. After degassing, light diffusion was no longer observed so that the sample was then considered to be homogeneous. Note that this clouding phenomenon was not observed in other RTILs where EuTf₃ was completely dissolved before degassing.

- (7) Oldham, W. J.; Costa, D. A.; Smith, W. H. In *Ionic liquids: industrial applications for green chemistry*; Rogers, R. D., Seddon, K. R., Eds.; American Chemical Society: Washington, DC, 2002; Vol. 15, p 188.
- (8) Bhatt, A. I.; May, I.; Volkovich, V. A.; Hetherington, M. E.; Lewin, B.; Thied, R. C.; Ertok, N. *J. Chem. Soc., Dalton Trans.* **2002**, 4532.
- (9) Billard, I.; Mekki, S.; Gaillard, C.; Hesemann, P.; Moutiers, G.; Mariet, C.; Labet, A.; Bünzli, J. C. *Eur. J. Inorg. Chem.* **2004**, 1190.
- (10) Chaumont, A.; Wipff, G. *Chem. Eur. J.* **2004**, *10*, 3919.
- (11) Chaumont, A.; Wipff, G. *Inorg. Chem.* **2004**, *43*, 5891.

- (12) Visser, A. E.; Swatloski, R. P.; Griffin, S. T.; Hatman, D.; Rogers, R. D. *Sep. Sci. Technol.* **2001**, *36*, 785.
- (13) Billard, I.; Moutiers, G.; Labet, A.; El Azzi, A.; Gaillard, C.; Mariet, C.; Lützenkirchen, K. *Inorg. Chem.* **2003**, *42*, 1726.

All samples were prepared at least 48 h before their analysis. All EXAFS and TRES experiments were performed at room temperature.

2.2. TRES Experiments. TRES experiments were performed with an excitation wavelength of 266 nm (Nd:YAG laser, 10 Hz, 6-ns pulse duration). The laser intensity was monitored with a powermeter (Scientech). The luminescence intensity as a function of time after excitation was selected via a monochromator and directed to a photomultiplier, connected to a fast oscilloscope. The laser setup was not corrected for light collection efficiency in the wavelength range investigated. The raw luminescence intensity at a given wavelength was obtained by integrating all corresponding counts. These data, plotted as a function of the emission wavelength in the range 585–630 nm, correspond to the raw emission spectrum of the sample. The wavelength precision of the monochromator is ± 0.25 nm, with a resolution on the order of ± 0.3 nm, but the emission spectra were recorded with 1-nm steps.

Because of the intense color of the BumimBF₄ solutions, indicative of organic impurities, and the resulting strong blue emission upon irradiation, it was not possible to obtain reliable results in this IL. Eu(III) solutions ($[\text{EuTf}_3] = 5 \times 10^{-4}$ M) were therefore studied by TRES in BumimTf, BumimPF₆, and BumimTf₂N liquids.

2.3. X-ray Absorption Spectroscopy. A summary of the samples investigated by XAFS spectroscopy is given in Table 1. After degassing, the liquid samples were placed in 0.4-mL sealed polyethylene vials. XAFS measurements were carried out at ANKA (Karlsruhe, Germany) on the XAS station and at the INE Beamline under normal storage ring conditions (2.5 GeV and 200–100 mA). Spectra were recorded at the Eu L_{III} edge (~ 6.977 keV) using a Si(311) water-cooled double-crystal monochromator at the XAS station and a Si(111) water-cooled double-crystal monochromator at the INE station. Both were calibrated in energy using the first inflection point in the K edge of an Fe foil, defined as 7.112 keV. Reference samples were measured in transmission using ionization chamber detectors. All RTIL samples were measured in fluorescence mode at room temperature using a five-element solid-state germanium detector (Canberra).

XAFS data reduction was carried out using the IFEFFIT code.¹⁴ The threshold energy, E_0 , was set to the first inflection point of the absorption edge. Data analysis was carried out with the FEFFIT code,¹⁵ using phase and backscattering amplitude functions generated with the FEFF 8.1 code¹⁶ for the model reference compounds Eu(H₂O)₉(Tf)₃,¹⁷ EuCl₃·6H₂O,^{18,19} and EuF₃. The crystallographic structure of EuF₃ is not clear, probably because EuF₃ may exist in two forms, orthorhombic and hexagonal, with the latter being noted to be stable only at elevated temperature. We chose the orthorhombic structure.^{20,21} The reliability of the phase and amplitude functions calculated by FEFF 8.1 was confirmed with spectra for the model reference compounds. Crystallographic parameters for Eu(H₂O)₉(Tf)₃ are 6 O at 2.40 Å and 3 O at 2.55 Å. EXAFS best-fit parameters: 6.4 \pm 0.8 O at 2.41(1) Å and 3.5 \pm 0.5 O at 2.57-

(1) Å. Crystallographic parameters for EuCl₃·6H₂O are 6 O at 2.43 Å and 2 Cl at 2.76 Å. EXAFS best-fit parameters: 6.6 \pm 0.8 O at 2.43(1) Å and 2.0 \pm 0.3 Cl at 2.76(1) Å. Crystallographic parameters for EuF₃ give 9 F at 2.36 Å. EXAFS best-fit parameters: 9.2 \pm 0.6 F at 2.34(1) Å.

Fits of the Fourier transform (FT) k^3 -weighted EXAFS data to the EXAFS equation were performed in R space between 1 and 3 Å. The k range used was 1.5–11.1 Å⁻¹. The amplitude reduction factor (S_0^2) was held constant to 1 for all fits. The shift in the threshold energy (E_0) was allowed to vary as a global parameter for all atoms in each of the fits. Estimated errors for the coordination number (CN) are $\pm 20\%$, for radial distance (R) ± 0.02 Å, and for the Debye–Waller factors (σ^2) ± 0.001 – 0.002 Å².

2.4. Computational Methods. 2.4.1. Molecular Dynamics. The different systems studied were simulated by classical MD using AMBER 7.0²² software, in which the potential energy U is described by a sum of the bond, angle, and dihedral deformation energies and a pairwise additive 1–6–12 (electrostatic and van der Waals) interaction between nonbonded atoms:

$$U = \sum_{\text{bonds}} k_b(r - r_0)^2 + \sum_{\text{angles}} k_\theta(\theta - \theta_0)^2 + \sum_{\text{dihedrals}} \sum_n V_n [1 + \cos(n\varphi - \gamma)] + \sum_{i < j} \left[\frac{q_i q_j}{R_{ij}} - 2\epsilon_{ij} \left(\frac{R_{ij}^*}{R_{ij}} \right)^6 + \epsilon_{ij} \left(\frac{R_{ij}^*}{R_{ij}} \right)^{12} \right] \quad (1)$$

Cross terms in van der Waals interactions were constructed using the Lorentz–Berthelot rules. The parameters used for the pure liquids were taken from De Andrade et al.²³ for the Bumim⁺ and BF₄⁻ ions, those for the PF₆⁻ anions were taken from the OPLS force field,²⁴ and those for Tf₂N⁻ were taken from the work of Lopes and Pádua.²⁵ These parameters have been shown to give good agreement with the experiment for the neat liquids. The atom types and charges are given in the Supporting Information (Figure S2).

The parameters for Eu³⁺ ($R^* = 1.852$ Å; $\epsilon = 0.05$ kcal/mol) have been fitted to the free energy of hydration.²⁶ Those for Tf⁻ come from the AMBER force field, and the Tf⁻ charges have been fitted to electrostatic potentials calculated at the HF/6-31G* level on the optimized structure and have previously been used to simulate lanthanide complexes.²⁷ The parameters of Cl⁻ ($R^* = 2.495$ Å; $\epsilon = 0.107$ kcal/mol) and F⁻ ions ($R^* = 1.850$ Å; $\epsilon = 0.20$ kcal/mol) have been fitted to their free energies of hydration.²⁸ Unless otherwise specified, they have been used throughout the study and named “big” Cl⁻ or F⁻ models. We also tested “smaller” anion models ($R^* = 1.943$ Å and $\epsilon = 0.265$ kcal/mol for Cl⁻; $R^* = 1.746$ Å and $\epsilon = 0.061$ kcal/mol for F⁻) taken from the AlCl₄⁻²³ and PF₆⁻²⁴ anion parameters, respectively.

The 1–4 van der Waals interactions were scaled down by a factor of 2.0, and the 1–4 Coulombic interactions were downscaled by

- (14) Newville, M. *J. Synchrotron Radiat.* **2001**, *8*, 322.
 (15) Newville, M.; Ravel, B.; Haskel, D.; Rehr, J. J.; Stern, A.; Yacoby, Y. *Physica B* **1995**, *208–209*, 154.
 (16) Ankudinov, A.; Rehr, J. J. *Phys. Rev. B* **2000**, *62* (4), 2437.
 (17) Harrowfield, J. M. B.; Kepert, D. L.; Patrick, J. M.; White, A. H. *Aust. J. Chem.* **1983**, *36*, 483.
 (18) Graeber, E. J.; Conrad, G. H.; Duliere, S. F. *Acta Crystallogr.* **1966**, *21*, 1012.
 (19) Bel'skii, N. K.; Struchkov, Y. T. *Sov. Phys. Cryst.* **1965**, *10*, 15.
 (20) Zalkin, A.; Templeton, D. H. *J. Am. Chem. Soc.* **1953**, *75*, 2453.
 (21) Zinchenko, V. F.; Efrushina, N. P.; Eryomin, O. G.; Markiv, V. Y.; Belyavina, N. M.; Mozkova, O. V.; Zakharenko, M. I. *J. Alloys Compd.* **2002**, *347*, L1.

- (22) Case, D. A.; Pearlman, D. A.; Caldwell, J. W.; Cheatham, T. E., III; Wang, J.; Ross, W. S.; Simmerling, C. L.; Darden, T. A.; Merz, K. M.; Stanton, R. V.; Cheng, A. L.; Vincent, J. J.; Crowley, M.; Tsui, V.; Gohlke, H.; Radmer, R. J.; Duan, Y.; Pitera, J.; Massova, I.; Seibel, G. L.; Singh, U. C.; Weiner, P. K.; Kollman, P. A. *AMBER 7*; University of California: San Francisco, 2002.
 (23) De Andrade, J.; Böes, E. S.; Stassen, H. *J. Phys. Chem. B* **2002**, *106*, 13344.
 (24) Kaminski, G. A.; Jørgensen, W. L. *J. Chem. Soc., Perkin Trans. 2* **1999**, 2365.
 (25) Lopes, J. N. C.; Pádua, A. A. H. *J. Phys. Chem. B* **2004**, *108*, 16893.
 (26) Van Veggel, F. C. J. M.; Reinhoudt, D. *Chem. Eur. J.* **1999**, *5*, 90.
 (27) Baaden, M.; Berny, F.; Madic, C.; Wipff, G. *J. Phys. Chem. A* **2000**, *104*, 7659.
 (28) Berny, F. Thesis, Université Louis Pasteur, Strasbourg, France, 2000.

1.2, as recommended by Cornell et al.²⁹ The pure liquids and solutions were simulated with three-dimensional-periodic boundary conditions. Nonbonded interactions were calculated using a 12-Å atom-based cutoff, correcting the long-range electrostatics by using the Ewald summation method in the particle-particle mesh Ewald approximation.

The MD simulations were performed at 300 and 400 K, starting with random velocities, using the Verlet leapfrog algorithm with a time step of 2 fs to integrate the equations of motion. The temperature was monitored by coupling the system to a thermal bath using the Berendsen algorithm³⁰ with a relaxation time of 0.2 ps. All C–H bonds were constrained using the Shake algorithm.

We first equilibrated “cubic” boxes of pure liquids of about 40-Å length, containing about 200 pairs of Bumim^+Y^- ions ($\text{Y}^- = \text{PF}_6^-$, BF_4^- , and Tf_2N^-). After equilibration, the solvent densities (1.33 g/cm³ for BumimPF_6 , 1.18 g/cm³ for BumimBF_4 and 1.49 g/cm³ for $\text{BumimTf}_2\text{N}$) were in reasonable agreement with the experimental data (1.36, 1.20, and 1.45 g/cm³, respectively).³¹ We then immersed one “naked” europium cation, removing Bumim^+ cations from the box to keep its total charge neutral. In each liquid, two other systems were also simulated, one with “complexed” triflates (forming intimate ion pairs with europium; hereafter noted as the EuTf_3 solute) and one with dissociated triflates (with triflate anions at about 15 Å from europium; hereafter noted as the $\text{Eu}^{3+}, 3\text{Tf}^-$ solute). The characteristics of the simulated systems are summarized in Table S1 of the Supporting Information. Equilibration started with 1500 steps of steepest-descent energy minimization, followed by 50 ps with fixed solutes (“BELLY” option in AMBER) at constant volume and by 50 ps without constraints at constant volume, followed by 50 ps at a constant pressure of 1 atm coupling the system to a barostat³⁰ with a relaxation time of 0.2 ps. Then MD was run for 4–5 ns in the NVT ensemble.

The MD trajectories were saved every 1 ps and analyzed with MDS and DRAW software.³² Typical snapshots were redrawn using VMD software.³³ The average structure of the solvent around Eu^{3+} was characterized by the radial distribution functions (RDFs) of the anions and cations during the last 0.2 ns. The average CN of the solvent anions (F and P atoms of PF_6^- , F and B atoms of BF_4^- , and O and N atoms of Tf_2N^-) and cations (N atom of Bumim^+) and its standard deviation were calculated up to a cutoff distance of the first peak of the RDF for the anion and up to 10 Å for the cation, for which the first peak is less well-defined. Insights into energy features were obtained by group component analysis, using a 17-Å cutoff distance and a reaction field correction for the electrostatics. In particular, the total potential energy of the system in solution was decomposed as $E = E_{\text{solute}} + E_{\text{solvent}} + E_{\text{ILIL}}$, where E_{solute} is the internal energy of the solute in solution, E_{solvent} is the solute/solvent interaction energy (“solvation energy”), and E_{ILIL} corresponds to the solvent/solvent interactions, calculated from the saved coordinates.

2.4.2. QM Calculations. The EuX_3 ($\text{X} = \text{F}^-$, Cl^- , Tf^- , PF_6^- , BF_4^- , and Tf_2N^-) and EuCl_6^{3-} complexes were optimized without symmetry constraints by QM calculations at the Hartree–Fock (HF)

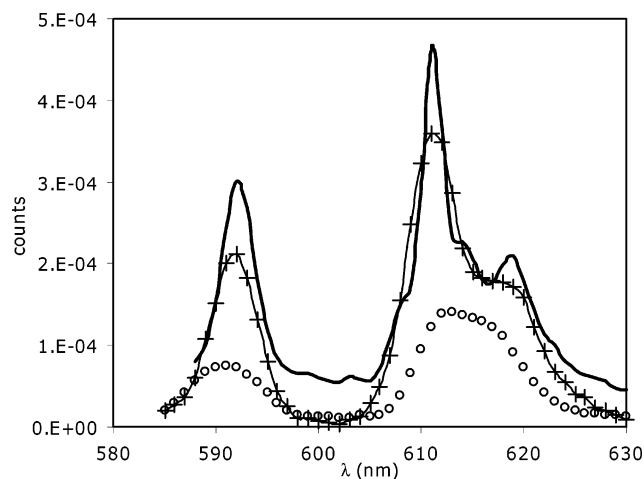


Figure 1. Emission spectra of Eu(III) : (thick solid line) $\text{EuCl}_6\text{Tf}_2\text{N}$; (○) EuTf ; (---) EuCl_6Tf . $\lambda_{\text{exc}} = 266$ nm.

and density functional (DFT; B3LYP functional) levels of theory, using *Gaussian 03* software.³⁴ Because f orbitals do not play a major role in metal–ligand bonds,³⁵ the 46 core and 4 f electrons of the Eu were described by the quasi-relativistic effective core potential^{36,37} of the Stuttgart group. For the valence orbitals, the affiliated (7s6p5d)/[5s4p3d] basis set was used, enhanced by an additional f function of exponent 0.591. For the C, N, O, F, B, P, and S atoms, we used 6-31+G* basis sets. The total energies are given in Table S2 of the Supporting Information.

3. Results

3.1. TRES Experiments. In the absence of chloride, the emission spectra of Eu(III) in the three investigated ILs $\text{BumimTf}_2\text{N}$, BumimTf , and BumimPF_6 are very similar, as is the emission spectrum of Eu(III) in the presence of chloride for $[\text{Cl}]/[\text{Eu}] = 6$ ($r = 6$) in BumimPF_6 . For the sake of clarity, only one of these four similar spectra is displayed in Figure 1. In contrast, in the presence of chloride anions, the emission spectra in BumimTf and $\text{BumimTf}_2\text{N}$ differ strongly, as shown in Figure 1.

In $\text{BumimTf}_2\text{N}$, both recorded spectra ($r = 0$ and 6) agree very well with our previously published results on this solvent.⁹ In the presence of chloride ions, by comparison

(34) Frisch, M. J.; Trucks, G. W.; Schlegel, H. B.; Scuseria, G. E.; Robb, M. A.; Cheeseman, J. R.; Montgomery, J. A., Jr.; Vreven, T.; Kudin, K. N.; Burant, J. C.; Millam, J. M.; Iyengar, S. S.; Tomasi, J.; Barone, V.; Mennucci, B.; Cossi, M.; Scalmani, G.; Rega, N.; Petersson, G. A.; Nakatsuji, H.; Hada, M.; Ehara, M.; Toyota, K.; Fukuda, R.; Hasegawa, J.; Ishida, M.; Nakajima, T.; Honda, Y.; Kitao, O.; Nakai, H.; Klene, M.; Li, X.; Knox, J. E.; Hratchian, H. P.; Cross, J. B.; Bakken, V.; Adamo, C.; Jaramillo, J.; Gomperts, R.; Stratmann, R. E.; Yazyev, O.; Austin, A. J.; Cammi, R.; Pomelli, C.; Ochterski, J. W.; Ayala, P. Y.; Morokuma, K.; Voth, G. A.; Salvador, P.; Dannenberg, J. J.; Zakrzewski, V. G.; Dapprich, S.; Daniels, A. D.; Strain, M. C.; Farkas, O.; Malick, D. K.; Rabuck, A. D.; Raghavachari, K.; Foresman, J. B.; Ortiz, J. V.; Cui, Q.; Baboul, A. G.; Clifford, S.; Cioslowski, J.; Stefanov, B. B.; Liu, G.; Liashenko, A.; Piskorz, P.; Komaromi, I.; Martin, R. L.; Fox, D. J.; Keith, T.; Al-Laham, M. A.; Peng, C. Y.; Nanayakkara, A.; Challacombe, M.; Gill, P. M. W.; Johnson, B.; Chen, W.; Wong, W.; Gonzalez, C.; Pople, J. A. *Gaussian 03*; Gaussian, Inc.: Wallingford, CT, 2004.

(35) Maron, L.; Eisenstein, O. *J. Phys. Chem. A* **2000**, *104*, 7140.

(36) Dolg, M.; Stoll, H.; Savin, A.; Preuss, H. *Theor. Chim. Acta* **1989**, *75*, 173.

(37) Dolg, M.; Stoll, H.; Savin, A.; Preuss, H. *Theor. Chim. Acta* **1993**, *85*, 441.

(29) Cornell, W. D.; Cieplak, P.; Bayly, C. I.; Gould, I. R.; Merz, K. M.; Ferguson, D. M.; Spelmeyer, D. C.; Fox, T.; Caldwell, J. W.; Kollman, P. A. *J. Am. Chem. Soc.* **1995**, *117*, 5179.

(30) Berendsen, H. J. C.; Postma, J. P. M.; Gunsteren, W. F. v.; DiNola, A. *J. Chem. Phys.* **1984**, *81*, 3684.

(31) Tokuda, H.; Hayamizu, K.; Ishii, K.; Susan, M. A. B.; Watanabe, M. *J. Phys. Chem. B* **2004**, *108*, 16593.

(32) Engler, E.; Wipff, G. In *Crystallography of Supramolecular Compounds*; Tsoucaris, G., Ed.; Kluwer: Dordrecht, The Netherlands, 1996; p 471.

(33) Humphrey, W.; Dalke, A.; Schulten, K. *J. Mol. Graphics* **1996**, *14*, 33.

with well-known emission spectra in methanol,³⁸ we ascribed this emission spectrum to an europium hexachloro, EuCl_6^{3-} , complex.

It is clear that in BumimTf the addition of chloride also modifies the Eu(III) emission, also indicative of complexation. However, because its emission is different from that observed for the BumimTf₂N plus chloride case, it is reasonable to assume that the hexachloro complex is not formed in BumimTf. The complex present in BumimTf is most probably of a lower stoichiometry than 1:6, but this limited study does not allow for a better determination. Finally, in C₄mimPF₆, the similarities between the emission spectra with and without chloride indicate the lack of any chloride complexation in this solvent.

In the case of BumimTf, some investigations on the lifetime values have been performed. First, it has been confirmed that the lifetimes are slowly decreasing through time once the degassed sample has been exposed to air, as was already observed for BumimTf₂N.⁹ However, the decrease is slow (by roughly 10% after 4 days of storage in the quartz cuvette closed with a Teflon cap) probably because of the slow introduction of water in the sample. It has also been confirmed that water introduction does not modify the shape of the emission spectra, up to 7 days. All of the emission spectra displayed in this work have been obtained readily after degassing of the samples. Second, the lifetime measured for Eu in BumimTf ($r = 0$) is equal to 255 μs and rises to 2300 μs after chloride introduction (readily after degassing in both cases). This last value is in rough agreement with that obtained for $r = 6$ in BumimTf₂N.⁹ The rather short value obtained for Eu alone ($r = 0$) in BumimTf may be ascribed to the presence of the impurities (see Section 2.1), which may interact with Eu as long as no chloride is present in the solution.

3.2. X-ray Absorption Spectroscopy. 3.2.1. XANES. XANES spectra are sensitive to the changes in the europium inner coordination sphere and therefore can be used to probe such changes. Figure 2 displays the Eu L_{III}-edge XANES spectra of the RTIL samples. The intense edge resonance or white line, positioned at 6983 eV, results from an electronic transition from a 2p_{3/2} core state to an empty 5d final state. The small feature at the high energy side of the white line between 6990 and 7000 eV is commonly attributed to multiple scattering contributions, and its energy position depends on europium's coordination structure and symmetry.^{39,40}

The addition of a chloride salt to the BumimPF₆ solution does not lead to significant changes in the Eu L_{III} XANES of the "EuPF₆" and "EuCl₆PF₆" samples, aside from a small reduction in the white-line amplitude (Figure 2a). In contrast, the BumimBF₄, BumimTf, and BumimTf₂N solutions (Figure 2b–d) exhibit changes in their spectral features upon the

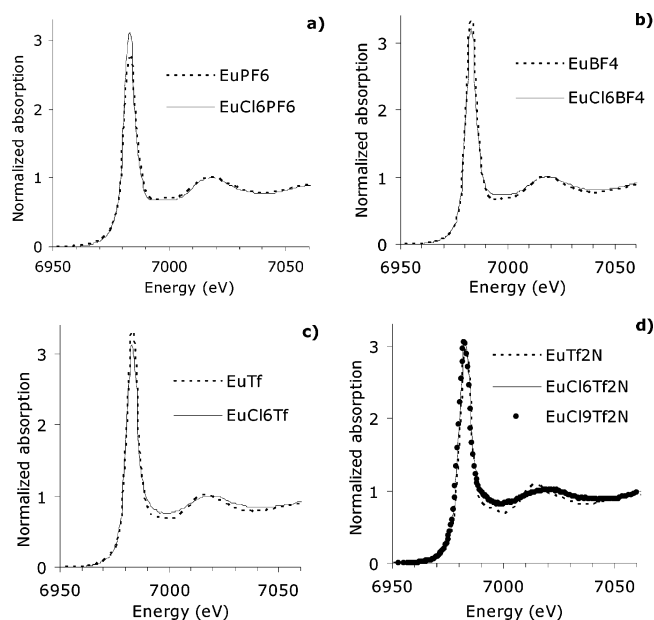


Figure 2. Eu L_{III} XANES spectra of Eu³⁺ dissolved in (a) BumimPF₆, (b) BumimBF₄, (c) BumimTf, and (d) BumimTf₂N, and for each RTIL, as a function of the chloride concentration. See Table 1 for an explanation of the sample designations.

addition of chloride ions. In particular, the shape, amplitude, and energy position of the first oscillation at ≈ 7020 eV are different and the feature at the high energy side of the white line disappears. These observations suggest that europium complexes added chloride anions in the BumimBF₄, BumimTf, and BumimTf₂N solutions but not in the BumimPF₆ solution, where the europium coordination sphere seems to remain unaffected upon chloride addition.

3.2.2. EXAFS. Figure 3 shows the k^3 -weighted EXAFS spectra and corresponding FT spectra obtained for the RTIL solutions. The FT peaks appear shifted to lower R values (~ 0.4 Å) as a result of the phase shift of the excited photoelectron as it travels through the absorber and surrounding atom potentials. As for the XANES region of the XAFS, we observe a spectral evolution for Eu(III) and the RTILs with and without chloride. The oscillatory frequency of the Eu L_{III} EXAFS increases after the addition of chloride, with the exception of the "EuPF₆" and "EuCl₆PF₆" samples. A frequency increase indicates a bond distance increase. This is evident in shifts of the main FT peak at 1.9 Å, corresponding to europium's first coordination sphere, following chloride addition (indicated with dotted lines in Figure 3b). Fit results to these data are given in Table 2.

The europium coordinations in "EuPF₆" and "EuBF₄" samples are similar, with approximately 9 F atoms at a distance near 2.35 Å. Fits to "EuTf" and "EuTf₂N" samples show europium to coordinate around 10 O atoms (within the experimental error) at approximately 2.42 Å.

As expected from qualitative inspection of the EXAFS and XANES data and TRES results, within the experimental error, fit results for the "EuPF₆" and "EuCl₆PF₆" samples are the same; the addition of a chloride salt into the Eu–BumimPF₆ solution does not lead to any significant change in the coordination structure. This indicates that no complexation occurs between europium and chloride ions in this

(38) Görrler-Wallrand, C.; de Moitié-Neyt, N.; Beyens, Y.; Bünzli, J. C. *J. Chem. Phys.* **1982**, *77*, 2261.

(39) Tan, Z.; Budnick, J. I.; Luo, S.; Chen, W. Q.; Cheong, S.-W.; Cooper, A. S.; Canfield, P. C.; Fisk, Z. *Phys. Rev. B* **1991**, *44* (13), 7008.

(40) Moreau, G.; Helm, L.; Purans, J.; Merbach, A. E. *J. Phys. Chem. A* **2002**, *106*, 3034.

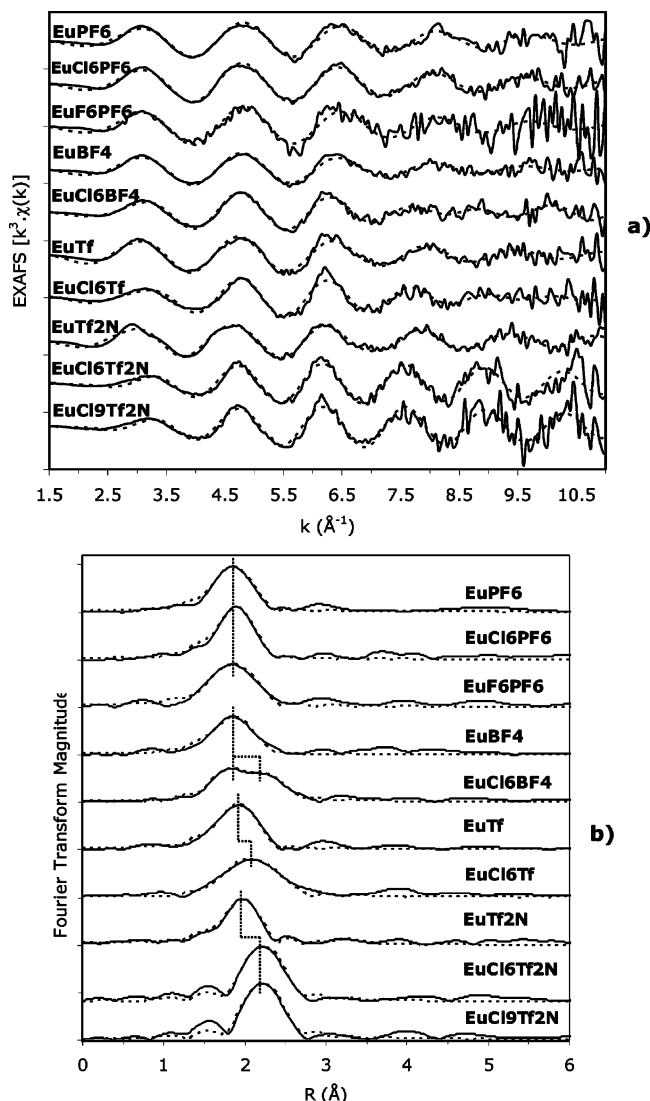


Figure 3. Eu L_{III}-edge k^3 -weighted EXAFS data (a) and corresponding FT spectra (not phase-shift-corrected) (b) for Eu^{3+} dissolved in RTIL and as a function of $[\text{Cl}^-]$: experimental data (—) and theoretical fit (---). See Table 1 for an explanation of the sample designations. Dotted lines in part b indicate the shifts of the main FT peak at 1.9 Å.

Table 2. EXAFS Structural Parameters for Eu^{3+} RTILs in Solution^a

sample ID ^b	shell	CN	σ^2 (Å ²)	R (Å)	E_0 (eV)	R factor
"EuPF ₆ "	Eu–F	8.9	0.009	2.34	–4.6	0.014
"EuCl ₆ PF ₆ "	Eu–F	10.1	0.009	2.36	–3.3	0.007
"EuF ₆ PF ₆ "	Eu–F	10.5	0.011	2.34	–4.4	0.025
"EuBF ₄ "	Eu–F	9.4	0.012	2.36	–3.7	0.014
"EuCl ₆ BF ₄ "	Eu–F	5.6	0.007	2.34	–4.7	0.007
	Eu–Cl	2.8	0.004	2.71		
"EuTf"	Eu–O	11.5	0.010	2.41	0.6	0.014
"EuCl ₆ Tf"	Eu–O	5.5	0.007	2.41	0.4	0.030
	Eu–Cl	3.5	0.007	2.73		
"EuTf ₂ N"	Eu–O	9.8	0.008	2.43	0.03	0.013
"EuCl ₆ Tf ₂ N"	Eu–Cl	6.9	0.006	2.69	–6.2	0.031
"EuCl ₉ Tf ₂ N"	Eu–Cl	5.9	0.004	2.67	–6.6	0.033

^a CN is the coordination number ($\pm 20\%$), σ^2 the Debye–Waller factor (± 0.001 – 0.002 Å²), R the interatomic distance (± 0.02 Å), and E_0 the shift in the threshold energy, and the R factor is the goodness of fit as defined in ref 15. ^b Defined in Table 1.

IL. This differs from the results for the BumimBF₄ solution, where the addition of chloride induces marked changes in both the EXAFS and FT spectra (compare the "EuBF₄" and

"EuCl₆BF₄" spectra and fit results; see Figure 3 and Table 2). In particular, a second nearest-neighbor contribution appears in the FT, centered at 2.3 Å. This splitting corresponds to partial replacement of F or O atoms by Cl atoms. Fit results show that there are 2.8 ± 0.6 Cl atoms at 2.71 ± 0.02 Å and 5.6 ± 1.1 F atoms at 2.34 ± 0.02 Å in "EuCl₆BF₄". Likewise, the addition of chloride to the BumimTf solution induces a shift and broadening of the FT main peak as a result of the replacement of O atoms coordinating europium by 3.5 ± 0.7 Cl atoms at 2.73 ± 0.02 Å. EXAFS results indicate that the addition of chloride to the BumimTf₂N solution leads to complete exchange of coordinated O atoms in "EuTf₂N" (without chloride) with 6–7 Cl atoms in samples "EuCl₆Tf₂N" and "EuCl₉Tf₂N". Because the EXAFS spectra of samples "EuCl₆Tf₂N" and "EuCl₉Tf₂N" are nearly identical, the saturated hexachloro complex likely forms in both samples when chloride is added. This corroborates the TRES results.

After dissolution of the triflate salt in the RTIL solutions, the CN for Eu(III) is found to be around 9–10, which is common for this lanthanide.⁴¹ A similar CN has been predicted by MD simulations on the "naked" Eu^{3+} cation immersed in the BumimPF₆ solution.⁴² According to these calculations, Eu(III) is solvated by 6 PF₆[–] ions, half in a monodentate fashion and half in a bidentate fashion, resulting in a CN of 9.8 ± 0.6 F. From our EXAFS study, the metal has a CN of 8.9 F in BumimPF₆ and of 9.4 F atoms in BumimBF₄, suggesting that Eu(III) is coordinated to solvent anions as found by MD.

In the presence of added chloride ions, the nature of Eu(III)'s first coordination sphere is found to depend on the nature of the RTIL because of the competition between the RTIL and the chloride anions as complexing ligands. Tf₂N[–] is the weakest complexant⁴³ of the anions we studied, so the halide complexation is complete in BumimTf₂N, leading to the formation of the EuCl_6^{3-} complex. BF₄[–] and Tf[–] are stronger complexing ligands, and in the BumimBF₄ and BumimTf solutions, mixed complexes are formed, likely involving less halogenated species such as EuCl_2^+ , EuCl_3 , and EuCl_4^- . In the BumimPF₆ solution, no chloride complexation occurs. This is, at first glance, surprising and might indicate a stronger affinity of europium for PF₆[–] than for chloride anions. This hypothesis seems, however, unlikely and is inconsistent with the theoretical results (vide infra).

An alternative explanation on the lack of chloride complexation in BumimPF₆ may be considered, based on the hypothesis that the first coordination sphere in this RTIL involves F[–] anions stemming, e.g., from Eu(III)-catalyzed decomposition of PF₆[–].⁴⁴ The complexed F[–] ions would prevent further Eu(III) complexation with chloride. Such an explanation is inconsistent, however, with MD results on

(41) Allen, P. G.; Bucher, J. J.; Shuh, D. K.; Edelstein, N. M.; Craig, I. *Inorg. Chem.* **2000**, *39*, 595.

(42) Chaumont, A.; Wipff, G. *Phys. Chem. Chem. Phys.* **2003**, *5*, 3481.

(43) Gaillard, C.; El Azzi, A.; Billard, I.; Bolvin, H.; Hennig, C. *Inorg. Chem.* **2005**, *44*, 852.

(44) Swatloski, R. P.; Holbrey, J. D.; Rogers, R. D. *Green Chem.* **2003**, *5*, 361.

$[\text{EuF}_n]^{3-n}$ complexes in the BumimPF₆ solution.⁴⁵ These MD simulations indeed find Eu(III) to bind 6 F⁻ anions at most, thereby forming the hexafluoro $[\text{EuF}_6]^{3-}$ complex. The same CN has also been observed spectroscopically for Eu(III) in molten salts⁴⁶ and is further supported by computational⁴⁷ and experimental observations of the $[\text{EuCl}_6]^{3-}$ analogue.^{48–50} In the BumimPF₆ solution, the spectroscopic observation of a CN of 9–10 indicates that europium is not complexed by F⁻ anions. Moreover, ³¹P NMR spectroscopy investigations on the “EuCl₆PF₆” sample and on the pure BumimPF₆ liquid did not detect phosphate ions, which would stem from the decomposition of PF₆⁻. Another piece of information comes from the EXAFS analysis of sample “EuF₆PF₆” with a relatively high fluoride salt concentration ratio ($[\text{F}]/[\text{Eu}] = 6$)⁵¹ showing that the coordination sphere of europium remains the same as that in the “EuPF₆” sample (see Figure 3 and Table 2). TRES analysis of the lifetime as a function of the irradiation time⁴³ (data not shown) further indicates that free fluoride ions are present in solution but do not complex. Thus, to summarize, when EuTf₃ is dissolved in the BumimPF₆ liquid, complexation of neither Cl⁻ nor F⁻ ions to europium is observed, despite the fact that these anions are stronger complexing ligands than PF₆⁻.

The above EXAFS analysis was performed assuming a total dissociation of the EuTf₃ salt introduced into the solution and coordination of Eu(III) by the IL anions only. Indeed, all RTIL solutions were clear and transparent after dissolution of the salts; no aggregate formation is observed. However, the state of EuTf₃ dissolved in the RTILs is not yet known and cannot be firmly assessed by EXAFS. Indeed, the “EuPF₆” spectrum could also be fitted with a mixed-shell model corresponding to the undissociated EuTf₃ salt, leading to a Eu coordination of 6.5 O atoms at 2.33 Å and 2.8 F atoms at 2.38 Å. On average, this distribution corresponds to the fit based on F atoms only (i.e., ≈9 F atoms at 2.34 Å). Actually, the EXAFS technique is not sensitive enough to safely discriminate between two light backscattering atom types such as oxygen and fluorine. One cannot, therefore, differentiate between nondissociated europium triflate moieties (involving Eu–O bonds) and their dissociated state (where Eu(III) is solvated by F atoms from the RTIL anions).

To summarize, EXAFS and TRES spectroscopic results point out the influence of the nature of the RTIL anions on the formation of halide complexes of europium. However, experimental data, combined with available theoretical results, do not explain the lack of Cl⁻ or F⁻ complexation by europium in BumimPF₆. For this reason, the environment of europium in RTILs has been investigated by MD and QM simulations. These results are presented in the following.

(45) Chaumont, A.; Wipff, G. *Phys. Chem. Chem. Phys.* **2005**, *7*, 1926.

(46) Dracopoulos, V.; Gilbert, B.; Papatheodorou, G. N. *J. Chem. Soc., Faraday Trans.* **1998**, *94*, 2601.

(47) Chaumont, A.; Wipff, G. *J. Phys. Chem. A* **2004**, *108*, 3311.

(48) Czjek, M.; Fuess, H.; Pabst, I. *Z. Anorg. Allg. Chem.* **1992**, *617*, 105.

(49) Matsumoto, K.; Tsuda, T.; Nohira, T.; Hagiwara, R.; Ito, Y.; Tamada, O. *Acta Crystallogr. C* **2002**, *C58*, m186.

(50) Mackenstedt, D.; Umland, W. Z. *Anorg. Allg. Chem.* **1993**, *619*, 1393.

(51) It was not possible to make a solution with a higher $[\text{F}]/[\text{Eu}]$ because of the solubility limit of the TBAF salt in BumimPF₆.

3.3. MD Simulations in ILs. Because the nature (intimate ion pairs versus fully dissociated ions) of the EuTf₃ salt in the RTILs is not known from experiment, we modeled both states, i.e., the “naked” Eu³⁺ cation and the EuTf₃ complex in three RTILs, focusing on the first coordination shell and the average CN of europium (obtained from the RDFs; see Figures 4 and 5 and Table S3 in the Supporting Information). The results are presented below, followed by an analysis of the energy features of the different systems, focusing on the state of the triflate counterions. Most MD simulations were carried out at 300 and 400 K to better enhance the dynamics, generally yielding similar results. Unless otherwise specified, the reported results correspond to a temperature of 300 K.

3.3.1. Solvation of “Naked” Eu³⁺ in BumimPF₆, BumimBF₄, and BumimTf₂N ILs. Two series of independent simulations were performed on the “naked” Eu³⁺ cation in three liquids. In an initial series (without triflate anions), neutrality was achieved by removing three Bumim⁺ ions from the solvent, whereas a second series involved the Eu³⁺, 3Tf⁻ solute with dissociated Tf⁻ anions. In both cases, the solvation of Eu³⁺ turned out to be nearly identical in a given IL. Therefore, we only report the first set of results.

In the BumimPF₆ solution, the Eu³⁺ cation is rapidly surrounded by 6 PF₆⁻ anions during the dynamics. These anions coordinate in either a mono- or bidentate fashion to the metal, as can be seen from the splitting of the first Eu–P_{PF₆} peak, leading to a total CN of 9.8 F atoms (Figure 4 and Table S3 in the Supporting Information). At 400 K, one more PF₆⁻ anion is coordinated to Eu³⁺, but the CN decreases to 9.2 F atoms because of the change from bi- to monodentate coordination of some anions.

When simulated in the BumimBF₄ liquid, Eu³⁺ rapidly (in less than 100 ps) coordinates BF₄⁻ anions to form a Eu(BF₄)₅²⁻ complex. The five anions are bidentate, leading to a total CN of 10.2 F atoms. At 400 K, Eu(BF₄)₅²⁻ takes up one more anion to form the Eu(BF₄)₆³⁻ complex in which the anions coordinate either monodentate (1.6 BF₄⁻) or bidentate (4.4 BF₄⁻) to Eu³⁺, leading to a CN of 10.4 F atoms.

In the BumimTf₂N solution, the Eu³⁺ cation rapidly coordinates five Tf₂N⁻ anions. Each anion binds in a bidentate fashion to the metal via one oxygen per SO₂ group, forming a six-membered ring chelate. Four Tf₂N⁻ ligands adopt a C_{2v}-type configuration with eclipsed CF₃ groups, whereas the fifth ligand is of C₂-type symmetry with a gauche arrangement of the CF₃ groups. This solvent shell remains unchanged when the system is heated to 400 K for 5 ns.

To summarize, the calculated CN for the “naked” Eu³⁺ cation ranges from 9.8 to 10.3 in the ILs, which is consistent with the EXAFS results. This does not prove, however, that the europium triflate salt is dissociated in a RTIL solution because similar CNs are obtained for undissociated EuTf₃ (vide infra).

3.3.2. Solvation of the Undissociated EuTf₃ Complex in the BumimPF₆, BumimBF₄, and BumimTf₂N ILs. The EuTf₃ complex was first optimized in the gas phase and

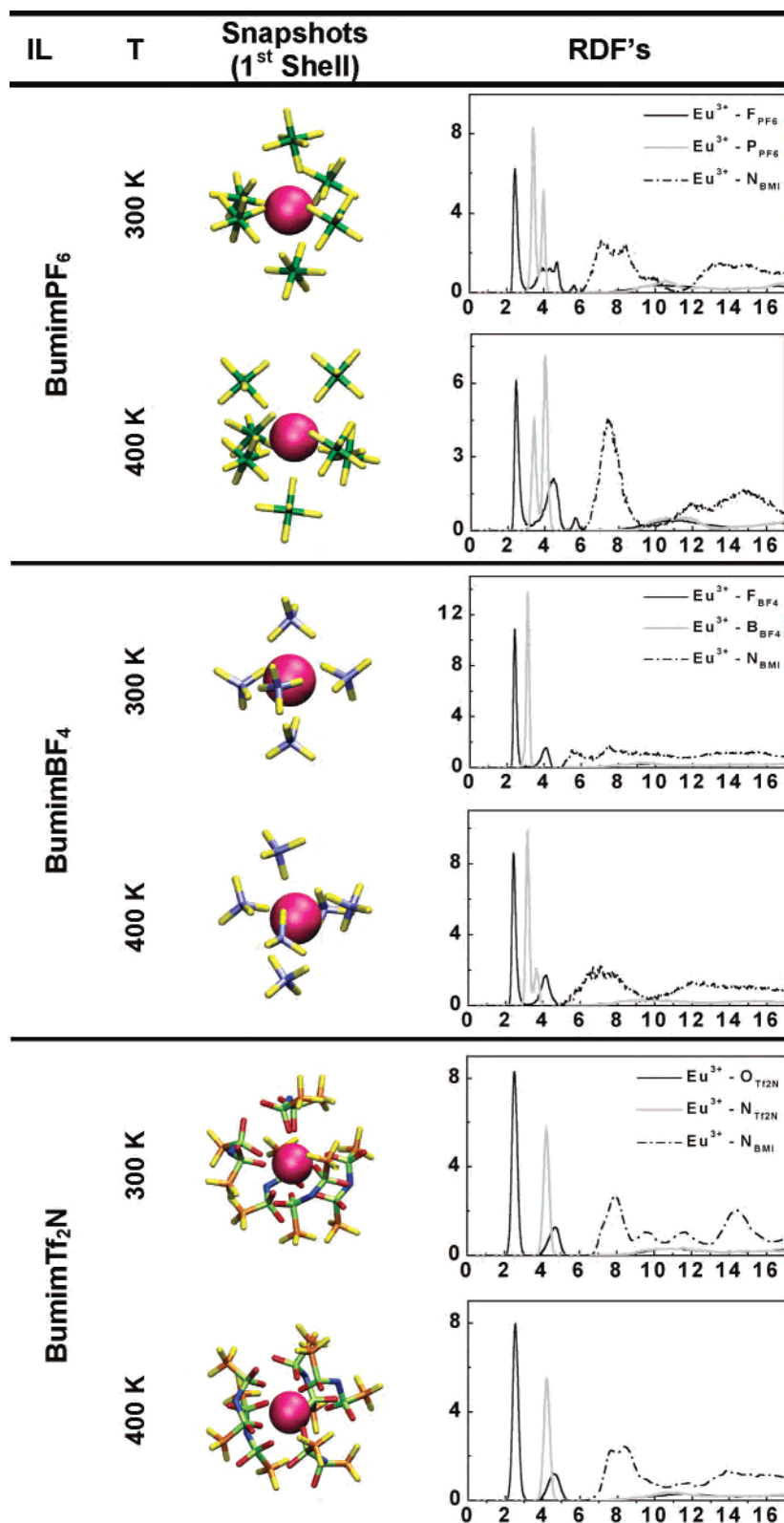


Figure 4. MD simulation for “naked” Eu^{3+} in different RTILs: snapshot of the first solvation shell around the cation and RDF of the solvent around the cation.

immersed in the different ILs. In no case did the complex dissociate during the dynamics, and the Tf^- anions remained bonded via their oxygen atoms to Eu^{3+} , with somewhat different denticities depending on the liquid. In the three liquids (BumimPF₆, BumimBF₄, and BumimTf₂N), the first

shell of Eu^{3+} is finally completed by two to three additional solvent anions, as described below.

In the BumimPF₆ solution, at 300 K the first coordination shell of Eu^{3+} comprises two monodentate PF_6^- anions. Because two Tf^- anions are tridentate and one is bidentate,

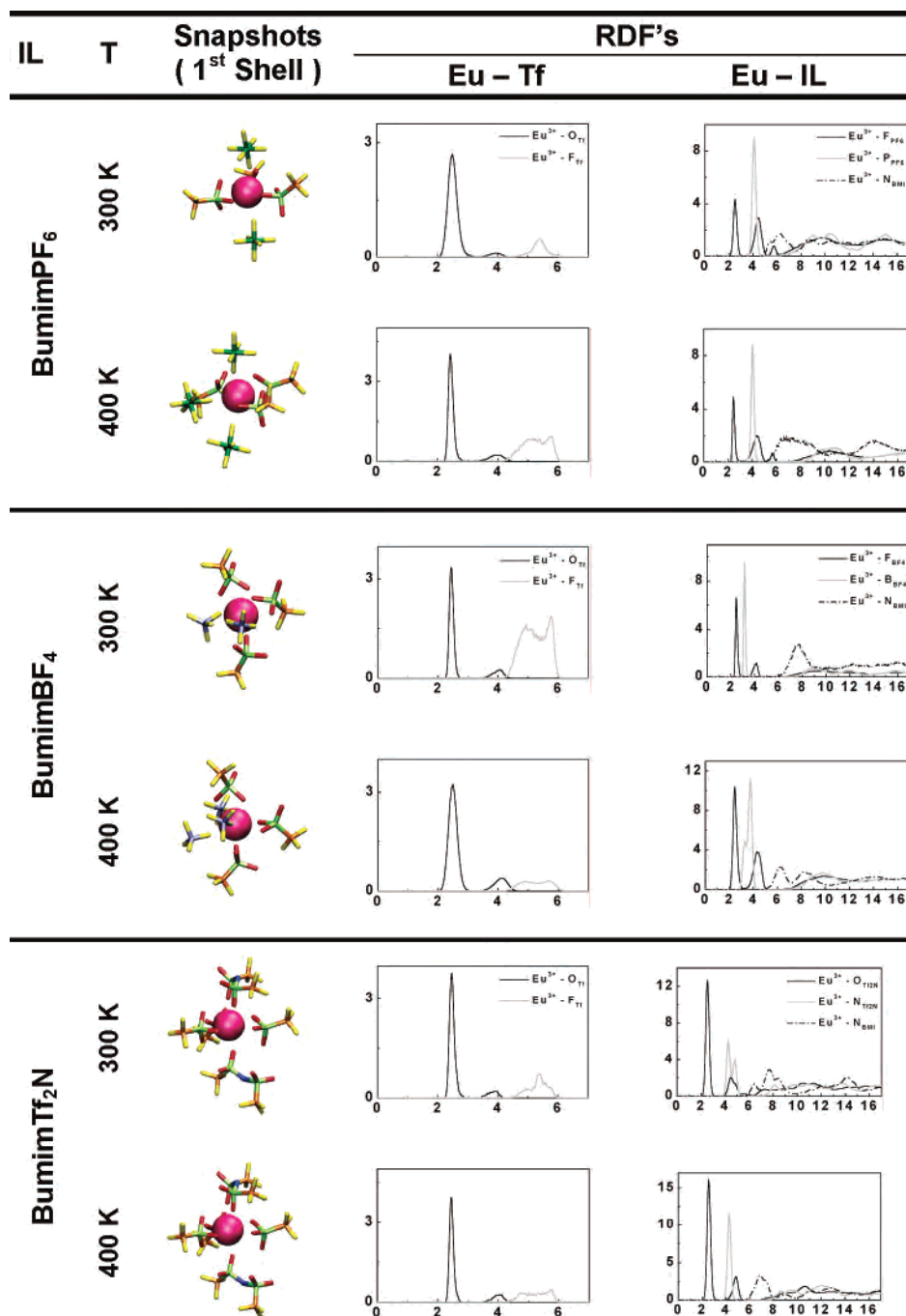


Figure 5. MD simulations for EuTf₃ in different RTILs: snapshot of the first solvation shell around the cation and RDF of the solvent around the cation.

the total average CN of Eu³⁺ is 9.8. Heating up the solution to 400 K leads to the capture of another PF₆⁻ after 1.7 ns, which is also coordinated monodentate to Eu³⁺. In this case, all Tf⁻ anions are bidentate, leading to a total CN of 9.1.

In the BumimBF₄ solution, the complex coordinated two BF₄⁻ anions after 0.25 ns of dynamics, and the resulting EuTf₃(BF₄)₂²⁻ complex remained stable until the end of the simulation. Both BF₄⁻ anions as well as all three Tf⁻ anions coordinate in a bidentate fashion to the metal, leading to a total CN of 10. After 3.8 ns at 400 K, the first shell is completed by another monodentate-coordinated BF₄⁻ anion, whereas one of the two other BF₄⁻ anions becomes monodentate and the other one remains bidentate. All three Tf⁻

anions coordinate bidentate to the cation, leading to a total CN of 9.7 atoms.

In the BumimTf₂N solution, the first coordination shell of europium is similarly completed by two Tf₂N⁻ anions, one being bidentate and forming a six-membered ring chelate and the other one monodentate. One of the three Tf⁻ ligands is tridentate and the other two are bidentate, leading to a total CN of 10.0. At 400 K, the monodentate and tridentate Tf₂N⁻ anions become bidentate, leaving the total CN of Eu³⁺ unchanged.

The predicted CN of the undissociated EuTf₃ complex in these ILs ranges from 9.1 to 10. Again this lies in the range of the EXAFS results. The knowledge of the total CN is

Table 3. Binding Energies (in kcal/mol) of EuX_3 Complexes Calculated by QM (6-31+G* Basis Set) at the HF or DFT-B3LYP Levels (with BSSE Correction) and Energy Minimized with AMBER, According to the Equation $\text{EuX}_3 \rightarrow \text{Eu}^{3+} + 3\text{X}^-$

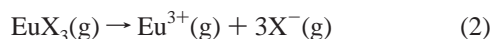
	HF	DFT-B3LYP	AMBER
EuF_3	1056	1075	1052 ^a (970) ^b
EuCl_3	911	953	936 ^a (836) ^b
EuTf_3	886	912	892
$\text{Eu}(\text{BF}_4)_3$	875	903	819
$\text{Eu}(\text{Tf}_2\text{N})_3$	869	891	726
$\text{Eu}(\text{PF}_6)_3$	843	875	697

^a Calculations performed with the “small” models for F^- and Cl^- .

^b Calculations performed with the “big” models for F^- and Cl^- .

thus not sufficient to conclude whether the europium salt is dissociated. Intermediate cases (e.g., EuTf^{2+} and EuTf_2^+ complexes) have not been simulated for time-saving purposes, but it can be surmised that they behave similarly, as far as the total CN is concerned.

3.3.3. Energy Analysis of the EuX_3 Complexes in the Gas Phase and in the RTIL Solutions. Relative Stabilities of EuX_3 Complexes in the Gas Phase. To compare the “intrinsic” binding strength of $\text{Eu}(\text{III})$ toward Y^- anions, we first performed QM calculations on EuY_3 complexes in the gas phase, comparing $\text{Y}^- = \text{F}^-, \text{Cl}^-, \text{BF}_4^-, \text{PF}_6^-, \text{Tf}^-$, and Tf_2N^- . The basis-set superposition error (BSSE)-corrected interaction energies ΔE_2 defined by eq 2 are given in Table 3 and compared to the force-field results. The QM results at



both DFT and HF levels follow the sequence $\text{F}^- > \text{Cl}^- > \text{Tf}^- > \text{BF}_4^- > \text{Tf}_2\text{N}^- > \text{PF}_6^-$. The same sequence is found with AMBER with the two models of F^- and Cl^- . The only exception concerns the Cl^- versus Tf^- ligands when Cl^- is described with the “big” model. The corresponding structures are given in Figure S3 in the Supporting Information, showing that PF_6^- and Tf^- bind bidentate (CN = 6). The Tf^- anions are coordinated via their SO_3^- oxygens. Attempts to optimize EuTf_3 complexes with a $\text{Eu}\cdots\text{F}(\text{Tf})$ coordination failed to converge, confirming the $\text{Eu}\cdots\text{O}(\text{Tf})$ type of binding, as found in solid-state structures.⁵² For the triflate anions, note the satisfactory agreement between the HF, DFT, and AMBER energies ($\Delta E_2 = 886, 912,$ and 892 kcal/mol).

The QM and AMBER calculations make clear that the $\text{Eu}(\text{PF}_6)_3$ complex is the least stable of the series, confirming that, intrinsically (i.e., in the gas phase), PF_6^- anions make weaker bonds with $\text{Eu}(\text{III})$ than Cl^- or F^- . Thus, the lack of Cl^- complexation when added to the BumimPF_6 solution should stem from other effects, as discussed below. According to the QM and AMBER results, there is no reason for the complexed Tf^- anions to be displaced by IL anions such as PF_6^- , Tf_2N^- , or BF_4^- . On the other hand, calculations predict all of these anions to be displaced by F^- and Cl^- in the gas phase.

Interactions of Eu^{3+} or EuTf_3 with the Solvents. The analysis of the interaction energy E_{solv} between Eu^{3+} or the EuTf_3 complex and the surrounding medium reveals interest-

Table 4. MD Simulations of an Uncomplexed Eu^{3+} Cation in IL Solutions (No Triflates): Average Cation Solvent Interaction Energies E_{solv} (in kcal/mol) and Their Components^a

IL	T (K)	BMI^+	Y^-	E_{solv}
BumimPF_6	300	1320 (18)	-2258 (20)	-938 (16)
	400	1475 (21)	-2422 (22)	-946 (20)
BumimBF_4	300	1493 (20)	-2567 (22)	-1073 (17)
	400	1638 (25)	-2730 (33)	-1092 (26)
$\text{BumimTf}_2\text{N}$	300	894 (14)	-1889 (19)	-995 (15)
	400	909 (24)	-1922 (24)	-1013 (17)

^a Fluctuations are given in parentheses.

Table 5. MD Simulations of the Undissociated EuTf_3 Complex in IL Solutions: Average Interaction Energy E_{solv} (in kcal/mol) between the Eu^{3+} , the IL, and Its Components and the Tf^- Anions^a

IL	T (K)	Tf^-	BMI^+	Y^-	E_{solv}
BumimPF_6	300	-978 (15)	1324 (18)	-1459 (19)	-1113 (18)
	400	-911 (14)	1359 (23)	-1584 (20)	-1136 (20)
BumimBF_4	300	-906 (10)	1543 (23)	-1778 (20)	-1141 (18)
	400	-894 (13)	1543 (23)	-1813 (28)	-1164 (24)
$\text{BumimTf}_2\text{N}$	300	-953 (10)	1025 (17)	-1205 (16)	-1132 (18)
	400	-906 (9)	1039 (16)	-1282 (16)	-1149 (15)

^a Fluctuations are given in parentheses.

ing trends, when one compares one liquid to the other. For the Eu^{3+} cation, the E_{solv} energies follow the same evolution as the ΔE_2 energies in EuX_3 complexes and increase from ≈ -940 kcal/mol for BumimPF_6 , -1000 kcal/mol for $\text{BumimTf}_2\text{N}$, and -1080 kcal/mol for BumimBF_4 (Table 4). This is consistent with the anionic nature of the first coordination shell of the “naked” cation in solution. For the EuTf_3 complex, the E_{solv} energies are closer to each other (see Table 5) because of weaker participation of solvent anions in the first europium shell.

Comparison of Complexed versus Dissociated Triflates in Solution. The state of triflate counterions in solution could, in principle, be investigated by performing potential of mean force calculations, which account for the change in free energy (ΔG) as a function of the $\text{Eu}\cdots\text{Tf}$ distances. Such approaches are presently too computationally demanding.



This is why we consider the dissociation reaction (3) in solution and compare the final and initial states in a given RTIL, simulated for 4 ns by MD in the same conditions at 300 and 400 K (Table S1 in the Supporting Information). Because the two states comprise the same numbers of solute and solvent particles, we can calculate the change in the total potential energies ΔU_3 for reaction (3) and analyze some key contributions: the internal energy of the solute (E_{solute}), the solute–solvent interactions (E_{solv}), and the solvent–solvent interactions (E_{ILIL}) in a given liquid. The averages over the last 0.5 ns are given in Table S4 in the Supporting Information and their differences in Table 6, showing similar trends at 300 and 400 K.⁵³

(53) Note that U was calculated “on the fly” directly during the MD simulation as an average over 500×500 configurations, whereas the E_{solute} , E_{solv} , and E_{ILIL} contributions were calculated from the saved trajectories as an average of 500×2 configurations. Thus, the sum $E = E_{\text{solute}} + E_{\text{solv}} + E_{\text{ILIL}}$ may not be identical with U . They are, however, within statistical fluctuations, similar.

(52) Hamidi, M.; Pascal, J.-L. *Polyhedron* **1994**, *13*, 1787.

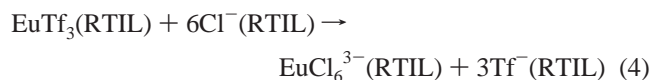
Table 6. Analysis of MD Simulations with Associated versus Dissociated Triflates [Reactions (3) and (4)]^a

RTIL	T (K)	ΔE_{solute}	ΔE_{solv}	ΔE_{IL}	ΔE	ΔU
EuTf ₃ → Eu ³⁺ + 3Tf ⁻ (3)						
BumimPF ₆	300	690	-1015	375	50	49
	400	649	-950	328	27	43
BumimBF ₄	300	702	-1213	412	-99	-109
	400	694	-1178	363	-121	-122
BumimTf ₂ N	300	697	-1096	317	-82	-101
	400	667	-1021	218	-136	-126
EuTf ₃ + 6Cl ⁻ → EuCl ₆ ³⁻ + 3Tf ⁻ (4)						
BumimPF ₆	400	-49	-77	-76	-202	-230
BumimTf ₂ N	400	-41	-71	49	-63	-56

^a Energy differences (in kcal/mol) are between the final and initial states. $\Delta E = \Delta E_{\text{solv}} + \Delta E_{\text{ILIL}} + \Delta E_{\text{solute}}$, where E_{solv} is the solute/solvent interaction energy, E_{ILIL} is the internal energy of the IL, and E_{solute} is the internal energy of the solute. The fluctuations of E_{solv} and E_{ILIL} are $\approx \pm 20$ and ± 70 kcal/mol, respectively. ΔU is the difference in potential energies between the final and initial states.⁵³ The corresponding fluctuations are about 50 kcal/mol.

In solution, dissociation of the triflates is favored by the better solvation of the Eu³⁺ and Tf⁻ ions, as indicated by the large gain in “solvation energies” ΔE_{solv} (from ≈ -950 to -1210 kcal/mol, depending on the liquid and on the temperature). Solvation of the dissociated ions is, however, detrimental to the solvent–solvent interactions, and the corresponding ΔE_{ILIL} changes range from 220 to 420 kcal/mol. Furthermore, bonding in the EuTf₃ complex is weakened in solution compared to the gas phase because of further coordination of Y⁻ solvent anions, and the complex is thus destabilized (by ≈ 200 kcal/mol if one compares to the ΔE_2 energies in the gas phase and the ΔE_{solute} energies in solution). Summing up these contributions ($\Delta E_3 = \Delta E_{\text{solv}} + \Delta E_{\text{ILIL}} + \Delta E_{\text{solute}}$) leads to positive energies in the BumimPF₆ liquid (≈ 40 kcal/mol) and to negative energies in the BumimBF₄ and BumimTf₂N liquids (≈ -100 kcal/mol). Thus, the change in the total energy ΔE_3 favors the complexed triflates in the BumimPF₆ solution and the dissociated triflates in the two other liquids. The same conclusions are obtained if one compares the total potential energy U of the systems with dissociated versus complexed triflates (Table S5 in the Supporting Information): ΔU_3 is positive in BumimPF₆ (40–50 kcal/mol) but negative in BumimBF₄ and BumimTf₂N (≈ -100 to -130 kcal/mol). This analysis is not intended to be quantitative because of the high fluctuations, force-field limitations, and entropic effects, which are unknown and not included. It does, however, point to the importance of solvation effects on the dissociation of the europium salt in the ILs. According to the MD simulations, the triflates should remain complexed in the RTIL, which contains fewer coordinating (PF₆⁻) anions, but dissociate in the other RTILs.

Comparison of Triflate versus Hexachloro Complexes of Europium in RTIL Solutions. Inspired by the experimental results, we modeled the exchange reaction (4) between the triflate salt (dissolved in the solution) and the hexachloro complex, whose occurrence was found experimentally to be solvent-dependent. The initial and final states



were independently simulated by MD for 4 ns in the BumimPF₆ and BumimTf₂N liquids at 400 K. The resulting E_{solv} , E_{ILIL} , and E_{solute} energies and their differences are given in Table 6. Results show that the formation of the hexachloro complex is favored by the change in the internal energy of the solute ($\Delta E_{\text{solute}} \approx -40$ to -50 kcal/mol, mainly because of the destabilization of the EuTf₃ moiety in solution)⁵⁴ and by the gain in solvation energies ($\Delta E_{\text{solv}} \approx -70$ to -80 kcal/mol), whereas the ΔE_{ILIL} contributions are more solvent-dependent. The net energies $\Delta E_4 = \Delta E_{\text{solv}} + \Delta E_{\text{ILIL}} + \Delta E_{\text{solute}}$ are negative (-200 kcal/mol in BumimPF₆ and -60 kcal/mol in BumimTf₂N), indicating that dissociation of the triflates to form the hexachloro complex is favored in the two liquids. The same conclusion is obtained if one compares the total potential energies of the initial and final states (see Table S6 in the Supporting Information): $\Delta U_4 \approx -230$ kcal/mol in BumimPF₆ and -55 kcal/mol in BumimTf₂N.⁵⁵

Thus, according to these results, the hexachloro complex of europium should form when EuTf₃ is dissolved in BumimPF₆ and BumimTf₂N liquids to which chloride anions have been added. We note that this conclusion contrasts the lack of experimental observation of the chloro complex in BumimPF₆ but is consistent with the observation of this complex in BumimTf₂N. Although computational results have to be examined with care, the comparisons of these QM versus AMBER results show that the AMBER results are reasonable.⁵⁶ Other validation tests have been reported in our previous work.^{10,11,45,47} The contradiction between simulation and experimental observation may, however, be understood if one considers that, in spite of the great care taken in the experiments, the kinetics of anion exchange around europium may be so slow that the systems examined by spectroscopy were not in thermodynamic equilibrium, as discussed below.

4. Discussion

Using spectroscopic techniques and theoretical calculations, we have investigated the influence of the RTILs' Y⁻ anions on the first coordination shell of a trivalent cation, europium(III), added as EuTf₃ salt. We first studied the triflate salt of europium dissolved in different “neat” RTILs. EXAFS gave a CN between 9 and 10 in each RTIL, as did MD simulations on a “naked” Eu³⁺ cation, as well as on the undissociated EuTf₃ complex. Spectroscopic data are not sufficient to characterize the state of the triflate counterions, but MD results suggest that the triflates should be complexed to europium in BumimPF₆ and dissociated in BumimBF₄ and BumimTf₂N solutions.

(54) In the gas phase, reaction (4) is calculated to be slightly endothermic (by $\Delta E_{\text{gas}} = 17, 20,$ and 15 kcal/mol, respectively according to the HF, DFT, and AMBER calculations; note the good agreement between the QM and force-field results).

(55) With the “small” Cl⁻ model, the corresponding values are also negative (-113 and -127 kcal/mol, respectively).

(56) We note that using the same theoretical approach and protocol to study the dissolution of the EuCl₃ salt in the BumimPF₆ solution ($\text{EuCl}_3 \rightarrow \text{Eu}^{3+} + 3\text{Cl}^-$), we correctly predict this process to be highly disfavored ($\Delta E = \Delta E_{\text{solv}} + \Delta E_{\text{ILIL}} + \Delta E_{\text{solute}} = 958 - 1181 + 770 = 547$ kcal/mol). This is fully consistent with the experimental observation (Billard, I.; Gaillard, C., unpublished).

Our studies of the europium solutions with added chloride or fluoride ions show that Eu(III) does not complex to these anions in the BumimPF₆ solution but more or less complexes Cl⁻ in the other RTILs. The lack of Cl⁻ or F⁻ complexation in the BumimPF₆ solution is quite puzzling because these anions should coordinate more strongly to Eu(III) than the triflate or solvent PF₆⁻ anions, which are, according to QM and MD results, the poorest ligands. The anomalous behavior of europium in BumimPF₆ might be related to the fact that EuTf₃, although dissolved in that RTIL, is not dissociated. In that solvent, however, as well as BumimTf₂N, the substitution of the coordinated triflates by Cl⁻ ligands to form the EuCl₆³⁻ complex should be energetically favored, according to the MD results. A fortiori, the corresponding EuF₆³⁻ complex should form in the presence of added F⁻ anions, but this is not observed by spectroscopy.

In the BumimBF₄ and BumimTf₂N solutions, europium is complexed by about 3 and 6 Cl⁻'s, respectively, and there is no simple explanation of these different stoichiometries as a function of the RTIL. In the studied samples, the Y⁻ RTIL anions, which compete with the Cl⁻ anions to coordinate to Eu(III), are in excess by a factor ranging from 14 in BumimPF₆ to 178 in BumimBF₄ (Table 1). We note, however, that the [Y⁻]/[Cl⁻] ratio does not follow the order of Cl⁻ complexation in the different liquids and that this concentration effect would favor, with everything else being the same, the complexation of chloride in BumimPF₆, which is contrary to the experiment. Furthermore, in a comparison of the BumimPF₆ and BumimTf₂N solutions, it is difficult to understand why 6 Cl⁻ anions are complexed to Eu(III) in the latter solution, whereas none is complexed in the former. The different stoichiometries of the chloro complexes can thus hardly be explained by concentration effects or by the intrinsic coordination properties of the solvent Y⁻ anions.

Note that in the studied series the fully halogenated hexachloro complex forms only in the BumimTf₂N liquid, which is less viscous than the others. In general, RTILs display rather high viscosities because of strong attractions between anions and cations. These high viscosities may affect the complexation rate of europium. In our case, we prepared samples for experiments at least 48 h before measurement. Solutions were mixed after introduction of the salts and the resulting solutions dried at 70 °C. This procedure may not be sufficient to reach equilibrium prior to analysis. According to the literature, the viscosities of the studied liquids at room temperature increase in the order^{2,57–59} BumimTf₂N (35–70 mPa) < BumimTf (≈90 mPa) < BumimBF₄ (150–220 mPa) < BumimPF₆ (240–450 mPa). The differences in these values are probably due to impurities or to different water contents (between 100 and 600 ppm), which significantly affects the viscosity.⁵⁹ It is likely not coincidental that this order is identical with the ordering of the reactivity of europium toward chloride we find experimentally. Thus,

(57) Pandey, S.; Fletcher, K. A.; Baker, S. N.; Baker, G. A. *Analyst* **2004**, *129*, 569.

(58) Seddon, K. R.; Stark, A.; Torres, M.-J. *Pure Appl. Chem.* **2000**, *72* (12), 2275.

(59) Widegren, J. A.; Laesecke, A.; Magee, J. W. *Chem. Commun.* **2005**, 1610.

differences in the rates of diffusion as a function of the anionic content of the RTILs, related to their viscosities, likely influence the nature of the observed complexes, especially in the case of dried solutions, where ion diffusion is slower than that in ones containing water. The addition of halide ions to the solution is also known to enhance the viscosity,⁵⁸ which may explain the lack of chloride and fluoride complexation in the BumimPF₆ solution.⁶⁰

In addition to slow ion diffusion, the energy barriers for anion exchange in the first coordination sphere of Eu(III) may be quite high in the RTIL and modulated by the nature of the europium counterions, RTIL anions, and added anions (e.g., halides). A recent study on the nucleophilic substitution of halides in Bumim-based RTILs⁶¹ revealed evidence for reduced halide nucleophilicities and higher activation energy barriers in RTILs than in conventional organic solvents. The rates of reaction in these liquids did not correlate with the RTILs' viscosities but rather with the halide solvation by the RTIL cation via hydrogen-bonding interactions. In our systems, the energy barriers should be much higher because (i) they involve the exchange of anions around a formally 3+ charged species with which they display strong attractions and (ii) the first anionic shell of the complex is shielded from the "bulk" solvent and stabilized by a shell of imidazolium cations, which renders the approach of an incoming anion more difficult.⁶¹

5. Conclusion

Solvation phenomena in RTILs are thus not as "simple" as those in classical solvents. The dissolution of, in our case, europium triflate salt, even if complete, does not imply dissociation and solvation of the metal cation by the RTIL anions only. The nature of the first coordination sphere of europium depends on the competition between its counteranions and the RTIL anions, which, in turn, influence the complexation reaction with other added anions such as chlorides. The europium counterions, initially present at the beginning of the experiment, although much less concentrated than the solvent anions, likely influence the complexation reaction and solvation process. The energy analysis of the MD trajectories makes clear that not only the nature of the first coordination shell but also solvation effects (includ-

(60) Another explanation may be found in the reaction of F⁻ anions with aromatic protons of Bumim⁺. We found indeed that, upon DFT/6-31+G* optimizations on the Bumim⁺F⁻ hydrogen-bonded adduct, the C₂H proton of Bumim⁺ spontaneously transferred to form the H–F molecule.

(61) Llewellyn, N.; Welton, T. *J. Org. Chem.* **2004**, *69*, 5986.

(62) The nature of the first coordination shell in solution cannot be predicted solely by a gas-phase approach, but looking beyond the first shell is not sufficient either. For instance, if one considers the interaction energy $E_{\text{solv}}(\text{Eu})$ of Eu(III) with its global environment in the RTIL solution when the cation is either "naked" Eu³⁺ or complexed with triflates (including in that case the contribution of the Tf⁻ anions), one sees (Tables 4 and 5) that, in the three studied liquids, $E_{\text{solv}}(\text{Eu})$ values are more negative with the complexed triflates in the three liquids (by ≈80 kcal/mol in BumimPF₆, 70 kcal/mol in BumimBF₄, and 40 kcal/mol in BumimTf₂N; averages over energies at 300 and 400 K). This would lead one to conclude that the triflates remain complexed by europium in all of these RTILs, which contrasts with the conclusions obtained in the BumimBF₄ and BumimTf₂N liquids when changes in solvent/solvent interactions (ΔE_{ILIL}) and in the internal energy of the solute (ΔE_{solute}) are taken into account.

ing the re-solvation of the dissociated ions and the change in the internal energy of the solutes and in the energy of the liquid itself) are important.⁶² Given the importance of the anionic components of the RTILs and of the dissolved europium salt, it can be expected that using other europium(III) salts will change its solvation and complexation properties, as well as the kinetics of anion exchange around the metal. Such experimental and theoretical studies are presently underway in our laboratories.

Acknowledgment. The authors acknowledge the ANKA Angstroemquelle Karlsruhe for beamtime allocation and thank Stefan Mangold, Kathy Dardenne, and Jörg Rothe for assistance using the ANKA-XAS and ANKA-INE beamlines. This work has been performed with the financial help of the

French "Groupement de Recherches" PARIS. IDRIS, CINES, and Université Louis Pasteur are acknowledged for contribution to computational resources.

Supporting Information Available: Tables of characteristics of simulated systems, total energies of the QM-optimized complexes, MD simulations of Eu^{3+} and EuTf_3 in RTILs and with associated versus dissociated triflates, and EuTf_3 versus Eu^{3+} , 3Tf and $\text{EuTf}_3, 6\text{Cl}^-$ versus EuCl_6^{3-} , 3Tf in different solutions and figures of residual water amount in $\text{Bumintf}_2\text{N}$ as a function of the degassing time, of AMBER atom types and charges used to simulate the RTILs and EuX_3 complexes in the gas phase. This material is available free of charge via the Internet at <http://pubs.acs.org>.

IC051055A